3-D Intraventricular Vector Flow Mapping Using Triplane Doppler Echo

Florian Vixège, Alain Berod, Franck Nicoud, Pierre-Yves Courand, Didier Vray, Damien Garcia

HAL Id: hal-03538680

https://hal-cnrs.archives-ouvertes.fr/hal-03538680

Submitted on 28 Jun 2022

3-D intraventricular vector flow mapping using triplane Doppler echo

Florian Vixège[1], Alain Berod[2,3], Franck Nicoud[3], Pierre-Yves Courand[1,4], Didier Vray[1], and Damien Garcia[1]

[1] CREATIS (Centre de Recherche en Acquisition et Traitement de l'Image pour la Santé), UMR5220, U1294 Lyon, France
damien.garcia@inserm.fr

[2] Sim&Cure, Montpellier, France
[3] IMAG, University of Montpellier, Montpellier, France
[4] Department of Cardiology, HCL, Lyon, France

https://www.biomecardio.com

Abstract. We generalized and improved our clinical technique of two-dimensional intraventricular vector flow mapping (2D-*i*VFM) for a full-volume three-component analysis of the intraventricular blood flow (3D-*i*VFM). While 2D-*i*VFM uses three-chamber color Doppler images, 3D-*i*VFM is based on the clinical mode of triplane color Doppler echocardiography. As in the previous two-dimensional version, 3D-*i*VFM relies on mass conservation and free-slip endocardial boundary conditions. For sake of robustness, the optimization problem was written as a constrained least-squares problem. We tested and validated 3D-*i*VFM *in silico* through a patient-specific heart-flow CFD (computational fluid dynamics) model, as well as *in vivo* in one healthy volunteer. The intraventricular vortex that forms during left ventricular filling was deciphered. After further validation, 3D-*i*VFM could offer clinically compatible 3-D echocardiographic insights into left intraventricular hemodynamics.

Keywords: Ultrasound imaging · Triplane doppler echo · 3-D vector flow imaging · Full-volume intracardiac blood flow

1 Introduction

1.1 The Intraventricular Diastolic Vortex

During the filling of the left ventricle (diastole), the valvular mitral inlet constrains the intraventricular blood flow to form a vortex. Although the geometry and orientation of the mitral valve contribute significantly to vortex formation and dynamics, the shape and relaxing deformations of the left ventricular cavity are the major contributors to vortex properties [1]. When heart filling is impaired (diastolic dysfunction), a change in blood flow occurs, with a significant impact on the intraventricular vortex [2]. Recent studies highlighted that quantification of the intraventricular blood flow

could improve the diagnosis of diastolic dysfunction, which often remains uncertain as standard echocardiographic indices may lead to divergent conclusions.

The clinical accessibility of echocardiography and its ability to provide non-invasive, real-time information make ultra-sound the preferred technique for analyzing the intra-cardiac blood flow at the bedside [3]. There are two main classes of methods for the analysis of blood flow by ultra-sound imaging: (1) techniques based on speckle tracking [4], such as echo-PIV (particle image velocimetry), and (2) approaches based on color Doppler, such as *i*VFM (intraventricular Vector Flow Mapping) [5]. Since speckle-tracking methods generally (but not necessarily [6]) require the injection of micro-bubbles [7], techniques derived from color-Doppler are preferable in clinical routine.

1.2 Full-Volume Three-Component by Conventional Color Doppler

Doppler echocardiography provides a scalar velocity field: it returns the velocity pro-jections along the ultrasound beams. Numerical methods were recently introduced to recover the three-dimensionality of intracardiac blood flow from color Doppler veloci-ties, such as multi-angle [8] or model-based [9] methods. Multi-angle techniques can be limited in a clinical context, as they require a series of acquisitions with different acous-tic windows. Model-based techniques rely on the optimization of an objective function based on hemodynamics (e.g., mass conservation). These 3-D studies were based on volume color Doppler, whose acquisitions are constrained by a compromise between spatial and temporal resolutions.

In the following section, we describe how we generalized our most recent version [10] of two-dimensional intraventricular vector flow mapping (2D-*i*VFM) in 3-D. The current 2D-*i*VFM technique is limited to the three-chamber apical long-axis view; it does not allow recovering the three-dimensional structure of intraventricular blood flow. With the objective of getting a full-volume three-component field:

(1) We used (and simulated) triplane Doppler echocardiographic images of a GE (Vivid e95) scanner, which gives access to three color Doppler planes (Fig. 2a) at a good temporal resolution.
(2) We modified the 2D-*i*VFM equations [10] for 3D-*i*VFM and made the numerical problem more robust by using a least-squares method with physics-based equality constraints.
(3) We determined the smoothing parameter automatically through the *L*-curve method [11] to make the regularization unsupervised and optimize operator independence.

2 Method – from Scalar Doppler to 3-D Vector Doppler

2.1 The Constrained Minimization Problem

The objective of 3D-*i*VFM is to reconstruct the actual 3-D intraventricular velocity field from triplane color Doppler. Triplane color Doppler returns three apical long-axis planes (color Doppler + B-mode) separated by an angle of $60°$ (Fig. 2a). We chose this triplane mode (rather than 3-D color Doppler) since (1) the ultrasound data

before scan-conversion are available through EchoPAC, and (2) the temporal resolution is higher. The Doppler (velocities) and B-mode (8-bit ultrasound image) data returned by the EchoPAC soft-ware are given in a spherical $\{r,\ \theta,\ \varphi\}$ coordinate system. Doppler velocity measured by echocardiography, $u_D(r,\ \theta,\ \varphi)$, is related to the radial velocity component, $v_r(r,\ \theta,\ \varphi)$, with a negative sign and additive noise η:

$$v_r(r,\theta,\varphi) \ = \ -u_D(r,\theta,\varphi) \ + \ \eta(r,\theta,\varphi). \tag{1}$$

The negative sign takes into account the color Doppler convention, which stipulates positivity when blood is directed towards the ultrasound array. The goal of 3D-iVFM is to determine the angular and azimuthal components in this spherical coordinate system, $v_\theta(r,\theta,\varphi)$ and $v_\varphi(r,\theta,\varphi)$, by using physics-based and smoothness constraints. The algorithm for 3D-iVFM is based on a generalized and improved version of the 2D-iVFM algorithm introduced by Assi $et\ al.$ [10]. We rewrote the problem as a constrained least-squares problem, which was solved by the Lagrange multiplier method. We used hemodynamic properties based on fluid dynamics to constrain the problem, such as mass conservation for an incompressible fluid (divergence-free flow), and free-slip boundary conditions on the endocardial wall. The minimization problem was mathematically written as

$$\vec{v}_{VFM} = \underset{\vec{v}}{\operatorname{argmin}} J(\vec{v}), \quad \text{with} \quad J(\vec{v}) = \int_\Omega (v_r \ + \ u_D)^2 \, \mathrm{d}\Omega + \alpha \mathcal{L}(\vec{v}) \tag{2}$$

subject to:

$$\begin{cases} \vec{v}_{VFM} \ \cdot \ \vec{n}|_{wall} \ - \ \vec{v}_{wall} \ \cdot \ \vec{n}|_{wall} \ = \ 0 \quad \text{on } \partial\Omega, \\ \qquad\qquad \operatorname{div}(\vec{v}_{VFM}) \ = \ 0 \quad \text{on } \Omega. \end{cases} \tag{3}$$

The velocity vectors $\vec{v}_{VFM}$ are the velocities recovered by color-Doppler Vector Flow Mapping, i.e. they are the solutions of the constrained minimization problem. The coordinates in the spherical system are $\{v_r(r,\theta,\varphi), v_\theta(r,\theta,\varphi), v_\varphi(r,\theta,\varphi)\}$. The second term in the cost function $J(\vec{v})$ in (2), namely $\mathcal{L}(\vec{v})$, stands for a spatial smoothing function that uses second-order partial derivatives, with cross-terms, with respect to the radial and angular coordinates (r,θ). The parameter α is the smoothing parameter (a scalar). Ω represents the intracavitary (intraventricular) region of interest, and $\partial\Omega$ is its endocardial (wall) boundary. $\vec{n}|_{wall}$ is the vector normal to the wall, and $\vec{v}_{wall}$ is the endocardial wall velocity. In the echocardiographic laboratory, the myocardial velocities can be derived, for example, by standard speckle tracking [4]. The first constraint equality in (3) describes the free-slip (no penetration) boundary conditions. Note that no-slip conditions are not recommended because the spatial resolution of color Doppler is not fine enough to capture the boundary layer. The second constraint equality in (3) represents the mass conservation for an incompressible fluid (divergence-free flow).

We applied the Lagrange multiplier method [12] and a finite-difference discretization to convert this constrained least-squares problem into a matrix form. To minimize operator dependence, we selected the smoothing parameter (α) automatically through the L-curve method [11]. A too-large parameter induces too much smoothing, a too-low parameter generates a noisy vector field. The best bias-variance compromise must be determined objectively.

2.2 Periodic Interpolation Along the Azimuthal Direction

Recalling that 3D-iVFM uses three long-axis planes (six azimuthal half-planes), we used a periodic trigonometric interpolation along the azimuthal direction to express the velocity vectors $\vec{v} = \{v_r, v_\theta, v_\varphi\}$ in (2). We thus wrote the three velocity components as follows:

$$
\begin{aligned}
v_k &= a0_k(r, \theta) + a1_k(r, \theta)\cos(\varphi) \\
&+ a2_k(r, \theta)\cos(2\varphi) + a3_k(r, \theta)\cos(3\varphi) \\
&+ a4_k(r, \theta)\sin(\varphi) + a5_k(r, \theta)\sin(2\varphi),
\end{aligned} \tag{4}
$$

with $k \in \{r, \theta, \varphi\}$.

It follows that the minimization problem (2) yields the coefficients aN_k, with $N = 0 \ldots 5$. These series of six coefficients correspond to the six half-planes given by triplane echocardiography. This interpolated expression ensures well-posedness of the problem and smoothness of each velocity component in the azimuthal direction. It also makes the numerical algorithm easily manageable in terms of memory and computation time (less than half a minute with a personal computer in Matlab language).

2.3 In Silico and in Vivo Analyses

We tested the 3D-iVFM algorithm (1) *in silico*, in a patient-specific 3-D dynamic model of intraventricular flow based on CFD (computational fluid dynamics) [13] (Fig. 1a), and (2) *in vivo*, in one healthy volunteer.

In Silico. The CFD model was already used to validate the previous 2D-iVFM version [10]. We used a patient-specific CFD cardiac model introduced by Chnafa *et al.* [13, 14]. In this CFD model, the heart chambers and wall dynamics were retrieved from 4D images acquired by computed tomography. An arbitrary Lagrangian-Eulerian (ALE) framework was adopted to handle the large amplitude motion of the cardiac tissues (endocardium and valves). This CFD model is detailed in several publications [13–15].

For the present study, triplane Doppler echo images were simulated by adding noise in the radial velocity components. Full-volume three-component velocity fields were estimated by 3D-iVFM (Eqs. 2–4), from these triplane Doppler velocities, and compared with the actual CFD velocity fields. Absolute errors and errors relative to the maximum speed were calculated (ground-truth CFD vs. 3D-iVFM).

In Vivo. As a clinical proof-of-concept, the left ventricle of one healthy volunteer was scanned by a cardiologist with a clinical ultrasound scanner (Vivid e95 GE), using the triplane color-Doppler mode (Fig. 2a). The Doppler and B-mode data before scan-conversion were extracted through the EchoPAC software (Fig. 2b). Full-volume three-component velocity fields were generated with 3D-iVFM (Eqs. 2–4).
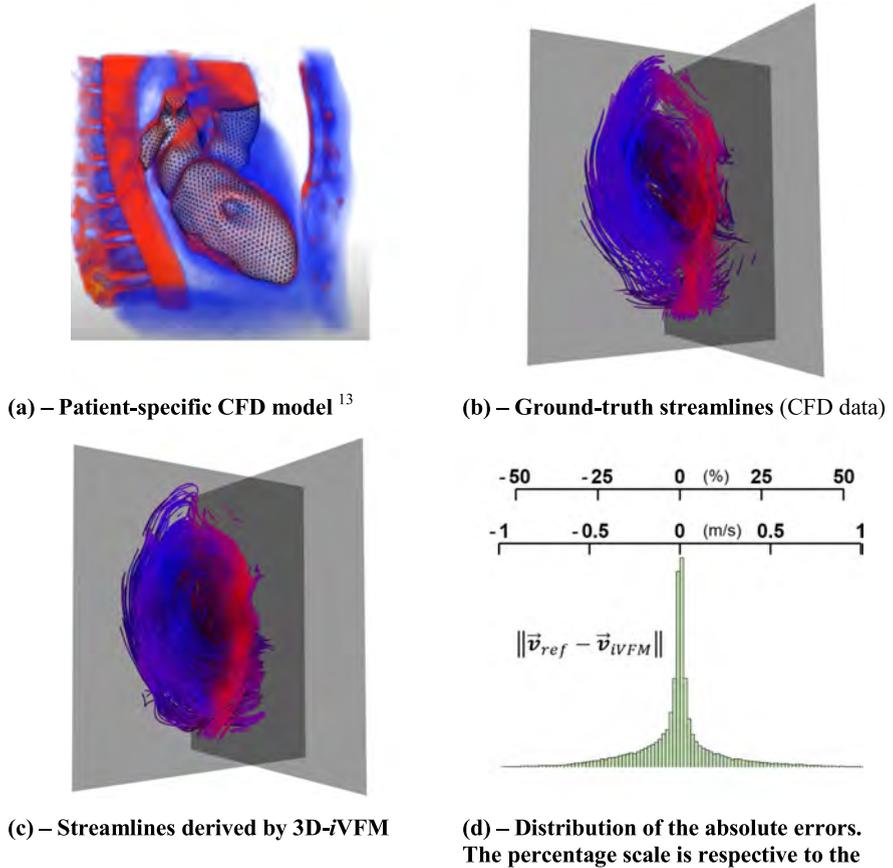
(a) – Patient-specific CFD model [13]

(b) – Ground-truth streamlines (CFD data)

(c) – Streamlines derived by 3D-*i*VFM

(d) – Distribution of the absolute errors. The percentage scale is respective to the

$$\|\vec{v}_{ref} - \vec{v}_{iVFM}\|$$

Fig. 1. *In silico results*: the streamlines (here, during filling) recovered after 3D-*i*VFM (c) were similar to the actual streamlines (b). The distribution of the absolute errors showed a narrow peak around zero (d).

3 Discussion

We successfully generalized 2D-*i*VFM for triplane Doppler echocardiography and introduced 3D-*i*VFM. Our *in silico* and *in vivo* one-case studies tend to show that 3D-*i*VFM could recover the 3-D structure of the intraventricular flow that forms during diastole. Although the 3-D intraventricular flow could not be recovered at small scales because of the smoothing regularizer present in the algorithm, our *in silico* results seem to show that a macroscopic 3D-flow analysis would be possible. For example, the global intraventricular circulation might reflect cardiac filling function. This remains to be demonstrated on a sufficiently large cohort of patients once the 3D-iVFM technique is finalized. The algorithm that we developed is fast and unsupervised, which makes it compatible with a

(a) –

Triplane Doppler echo
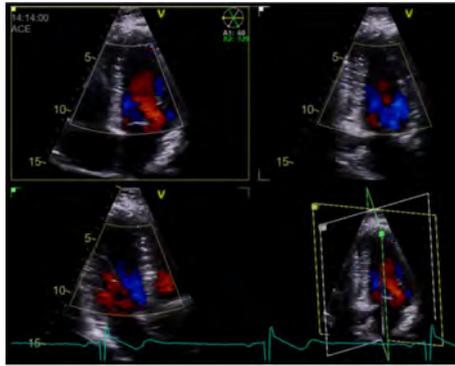
(b) –

Doppler data input for 3D-_i_VFM
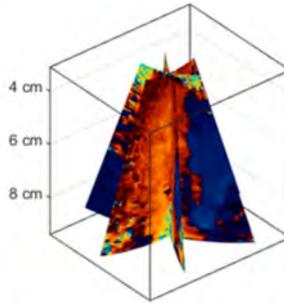
(c) –

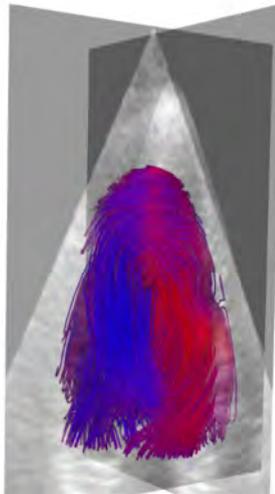**_In vivo_ streamlines derived by 3D-_i_VFM**

Fig. 2. _In vivo observation_: our innovative 3D-_i_VFM clinical method uses triplane Doppler echocardiography (a). The streamlines recovered by 3D-_i_VFM from the triplane Doppler velocities (b) depicted the large vortex that formed during filling (c).

standard examination in the echocardiographic laboratory. It depends on a single regularization parameter, which was selected automatically. This numerical aspect is important

to minimize operator dependence. Further *in vivo* investigation is planned to compare 3D-*i*VFM against CMR (cardiac magnetic resonance) velocimetry in patients, as in [16].

This study complements our *in vivo* analyses of intra-ventricular flow by color Doppler, whether by conventional [10, 17], or high-frame-rate echocardiography [18, 19]. In the present study, we opted for standard ultrasonography to facilitate a possible future clinical study. For this reason, we used a triplane mode. This mode has two specificities: (1) the temporal resolution is higher than that of 3-D Doppler, and (2) the acquired data can be extracted through EchoPAC for post-processing by *i*VFM (as opposed to 3-D data) [10, 20]. Although this needs to be quantified, it is likely that access to volume data, rather than triplane data, could reduce the bias of the reconstructed velocities. Whether this difference in bias is significant from a physiological point of view needs to be analyzed.

4 Conclusion

Intracardiac velocimetry by 3D-*i*VFM could be an effective tool for quantifying the intra-ventricular vortex and for assessing blood flow during heart filling. Fast and clinically compatible, 3D-*i*VFM could offer new echocardiographic insights into left ventricular hemodynamics

References

1. Charonko, J.J., Kumar, R., Stewart, K., Little, W.C., Vlachos, P.P.: Vortices formed on the mitral valve tips aid normal left ventricular filling. Ann. Biomed. Eng. **41**(5), 1049–1061 (2013). https://doi.org/10.1007/s10439-013-0755-0
2. Bermejo, J., Martínez-Legazpi, P., del Álamo, J.C.: The clinical assessment of intraventricular flows. Annu. Rev. Fluid Mech. **47**(1), 315–342 (2015). https://doi.org/10.1146/annurev-fluid-010814-014728
3. Sengupta, P.P., Pedrizzetti, G., Kilner, P.J., et al.: Emerging trends in CV flow visualization. JACC: Cardiovascul. Imaging **5**(3), 305–316 (2012). https://doi.org/10.1016/j.jcmg.2012.01.003
4. Garcia, D., Saloux, E., Lantelme, P.: Introduction to speckle tracking in cardiac ultrasound imaging. In: Handbook of Speckle Filtering and Tracking in Cardiovascular Ultrasound Imaging and Video. Institution of Engineering and Technology (2017)
5. Garcia, D., del Álamo, J.C., Tanné, D., et al.: Two-dimensional intraventricular flow mapping by digital processing conventional color-Doppler echocardiography images. IEEE Trans. Med. Imaging **29**(10), 1701–1713 (2010). https://doi.org/10.1109/TMI.2010.2049656
6. Nyrnes, S.A., Fadnes, S., Wigen, M.S., Mertens, L., Lovstakken, L.: Blood speckle-tracking based on high–frame rate ultrasound imaging in pediatric cardiology. J. Am. Soc. Echocardiogr. (2020). https://doi.org/10.1016/j.echo.2019.11.003

7. Hong, G.-R., Pedrizzetti, G., Tonti, G., et al.: Characterization and quantification of vortex flow in the human left ventricle by contrast echocardiography using vector particle image velocimetry. JACC: Cardiovascul. Imaging **1**(6), 705–717 (2008). https://doi.org/10.1016/j.jcmg.2008.06.008

8. Gomez, A., Pushparajah, K., Simpson, J.M., Giese, D., Schaeffter, T., Penney, G.: A sensitivity analysis on 3D velocity reconstruction from multiple registered echo Doppler views. Med. Image Anal. **17**(6), 616–631 (2013). https://doi.org/10.1016/j.media.2013.04.002

9. Grønli, T., Wigen, M., Segers, P., Lovstakken, L.: A fast 4D B-spline framework for model-based reconstruction and regularization in vector flow imaging. In: 2018 IEEE International Ultrasonics Symposium (IUS), pp. 1–9 (2018). https://doi.org/10.1109/ultsym.2018.8579767

10. Assi, K.C., Gay, E., Chnafa, C., et al.: Intraventricular vector flow mapping-a Doppler-based regularized problem with automatic model selection. Phys. Med. Biol. **62**(17), 7131–7147 (2017). https://doi.org/10.1088/1361-6560/aa7fe7

11. Hansen, P.C.: The L-curve and its use in the numerical treatment of inverse problems. In: Johnston, p. (ed.) Computational Inverse Problems in Electrocardiology. Advances in Computational Bioengineering, pp. 119–142. WIT Press (2000)

12. Kalman, D.: Leveling with Lagrange: an alternate view of constrained optimization. Math. Mag. **82**(3), 186–196 (2009)

13. Chnafa, C., Mendez, S., Nicoud, F.: Image-based large-eddy simulation in a realistic left heart. Comput. Fluids **94**, 173–187 (2014). https://doi.org/10.1016/j.compfluid.2014.01.030

14. Chnafa, C., Mendez, S., Nicoud, F.: Image-based simulations show important flow fluctuations in a normal left ventricle: what could be the implications? Ann. Biomed. Eng. **44**(11), 3346–3358 (2016). https://doi.org/10.1007/s10439-016-1614-6

15. Chnafa, C., Mendez, S., Moreno, R., Nicoud, F.: Using image-based CFD to investigate the intracardiac turbulence. In: Quarteroni, A. (ed.) Modeling the Heart and the Circulatory System. M, vol. 14, pp. 97–117. Springer, Cham (2015). https://doi.org/10.1007/978-3-319-05230-4_4

16. Faurie, J., Baudet, M., Assi, K.C., et al.: Intracardiac vortex dynamics by high-frame-rate Doppler vortography – in vivo comparison with vector flow mapping and 4-D flow MRI. IEEE Trans. Ultrason. Ferroelectr. Freq. Control **64**(2), 424–432 (2017)

17. Mehregan, F., Tournoux, F., Muth, S., et al.: Doppler vortography: a color Doppler approach to quantification of intraventricular blood flow vortices. Ultrasound Med. Biol. **40**(1), 210–221 (2014). https://doi.org/10.1016/j.ultrasmedbio.2013.09.013

18. Faurie, J., Baudet, M., Poree, J., Cloutier, G., Tournoux, F., Garcia, D.: Coupling myocardium and vortex dynamics in diverging-wave echocardiography. IEEE Trans. Ultrason. Ferroelectr. Freq. Control **66**(3), 425–432 (2019). https://doi.org/10.1109/TUFFC.2018.2842427

19. Garcia, D., Kadem, L., Savéry, D., Pibarot, P., Durand, L.-G.: Analytical modeling of the instantaneous maximal transvalvular pressure gradient in aortic stenosis. J. Biomech. **39**(16), 3036–3044 (2006). https://doi.org/10.1016/j.jbiomech.2005.10.013

20. Muth, S., Dort, S., Sebag, I.A., Blais, M.-J., Garcia, D.: Unsupervised dealiasing and denoising of color-Doppler data. Med. Image Anal. **15**(4), 577–588 (2011). https://doi.org/10.1016/j.media.2011.03.003